Journal of Oceanography, Vol. 60, pp. 905 to 912, 2004

Merging Satellite Infrared and Microwave SSTs: Methodology and Evaluation of the New SST

Lei Guan[1,2]* and Hiroshi Kawamura[1]

[1]*Center for Atmospheric and Oceanic Studies, Graduate School of Science, Tohoku University, Sendai 980-8578, Japan*
[2]*Ocean Remote Sensing Institute, Ocean University of China, Qingdao 266003, China*

(Received 13 May 2002; in revised form 22 December 2003; accepted 22 December 2003)

The Global Ocean Data Assimilation Experiment (GODAE) requires the availability of a global analyzed SST field with high-resolution in space (at least 10 km) and time (at least 24 hours). The new generation SST products would be based on the merging of SSTs from various satellites data and *in situ* measurements. The merging of satellite infrared and microwave SST data is investigated in this paper. After pre-processing of the individual satellite data, objective analysis was applied to merge the SST data from NOAA AVHRR (National Oceanic and Atmospheric Administration, Advanced Very High Resolution Radiometer), GMS S-VISSR (Geostationary Meteorological Satellite, Stretched-Visible Infrared Spin Scan Radiometer), TRMM MI (Tropical Rainfall Measuring Mission, Microwave Imager: TMI) and VIRS (Visible and Infrared Scanner). The 0.05° daily cloud-free SST products were generated in three regions, viz., the Kuroshio region, the Asia-Pacific Region and the Pacific, during one-year period of October 1999 to September 2000. Comparisons of the merged SSTs with Japan Meteorological Agency (JMA) buoy SSTs show that, with considerable error sources from individual satellite data and merging procedure, an accuracy of 0.95 K is achieved. The results demonstrate the practicality and advantages of merging SST measurements from various satellite sensors.

Keywords:
· SST,
· infrared,
· microwave,
· objective analysis,
· merge.

1. Introduction

The Global Ocean Data Assimilation Experiment (GODAE) is an international endeavor to develop operational ocean analysis and prediction systems for the global ocean. It requires an operational high resolution sea surface temperature (SST) product. This product would have a resolution near or better than 10 km, a temporal resolution of 24 hours or less, and include proper account of skin temperature effects. It would be based on data from several different remote sensing instruments, appropriately calibrated against direct measurements (prospectus for a *GODAE SST Project, 2000*; http://www.bom.gov.au/bmrc/ocean/GODAE/HiResSST/index.html).

Satellite SST has been available for about thirty years. The Advanced Very High Resolution Radiometers (AVHRR) on board National Oceanic and Atmospheric Administration (NOAA) polar-orbiting operational environmental satellites have provided operational SST observations for two decades (Kidwell, 1998; Goodrum *et al*., 2000). Two satellites constantly measure the surface four times per day with a spatial resolution of 1.1 km. The rms error of AVHRR-derived SST for the global coverage is about 0.6–0.7 K (Strong and McClain, 1984; McClain, 1989). The accuracy of regional SST around Japan is 0.6 K (Sakaida and Kawamura, 1992). SST estimation from the Stretched-Visible Infrared Spin Scan Radiometer onboard Geostationary Meteorological Satellite (S-VISSR, GMS), has been improved with a new algorithm to an rms error of about 0.8 K (Tanahashi *et al*., 2000). The unique advantage of geostationary satellite measurements is their high temporal resolution (30 minutes–1 hour), which enables us to resolve diurnal SST variations (Legeckis and Zhu, 1997; Wu *et al*., 1999). Although there are many advantages of the operational infrared SST measurements, the applications of the data are severely limited by the presence of clouds. Accurate satellite SST measurements under clouds have been available since the launch of Tropical Rainfall Measuring Mission (TRMM), which carried the Microwave Imager (hereafter, referred to TMI). The microwaves can penetrate clouds and the TMI 10 GHz bands are sensitive to

* Corresponding author. E-mail: leiguan@orsi.ouc.edu.cn

Copyright © The Oceanographic Society of Japan.

Table 1. Specifications of the satellite data.

Satellite sensor	Spatial resolution	Temporal resolution	Coverage	Accuracy (K)
NOAA AVHRR	0.01°	Twice per day per satellite	20°N~ 60°N 120°E~160°E	0.6
GMS S-VISSR	0.05°	Hourly	20°N~ 60°N 120°E~160°E	0.8
TRMM MI	0.25°	Three days for full coverage	38°S~38°N 0°~ 360°E	0.7
TRMM VIRS	0.05°	Three days for full coverage	38°S~38°N 0°~ 360°E	0.7

SST variations. The TMI-derived SST has an rms error of about 0.6–0.7 K (Shibata *et al.*, 1999; Wentz *et al.*, 2000; Kachi *et al.*, 2001). However, the spatial resolution of TMI SST is much lower, about 50 km.

Quantitative investigation of the SST availabilities of infrared and microwave measurements shows that the annual-mean availabilities of AVHRR, S-VISSR and TMI are 48%, 56% and 78%, respectively in the ocean south of Japan (Guan and Kawamura, 2003). The microwave measurements provide SST information at a constant high rate of 70–80% in the mid-latitude oceans, while the infrared measurements are disturbed by cloud coverage. By combining the advantages of high-availability TMI SST, high-spatial resolution AVHRR SST, and high-temporal resolution S-VISSR SST, it is feasible to generate cloud-free high-resolution SST.

The satellite SSTs used in the present study are all tuned against the *in situ* SSTs. It is well known that the bulk SSTs sometime differ from the skin SSTs, which is one of the problems in terms of the satellite SST measurements (e.g., Schlüessel *et al.*, 1990; Donlon *et al.*, 2002). However, in the present study we only discuss the merging methodology of the satellite SSTs tuned against common *in situ* SSTs observed by the drifting buoys. Therefore, the bulk-skin differences are not our concern here.

However, even the buoy SSTs (the satellite SSTs tuned against the buoy SSTs) have diurnal variations (e.g., Tanahashi *et al.*, 2003; Kawai and Kawamura, 2003), which is recognized as one of the important aspects of SST merging (Kawamura, 2002). Dealing with the SST diurnal variation properly is essentially important to produce high-quality daily SST products through merging various satellite SSTs observed at different times in a day. Kawamura (2002) proposed a correction method of diurnal SST variations for the satellite SST merging, which is to tune each satellite SST in a day to the daily minimum or the daily mean SST using information of satellite insolation, wind speeds, etc. If we can use many satellite SSTs with different acquisition times in a day, the daily mean SST can be obtained easily.

The purpose of this study is to investigate the methodology and demonstrate the practicality of the merged SST from infrared and microwave measurements. Since we could use many satellite SSTs (a rough estimate of the maximum overpass for a point is about 30) in this study, the derived merged products can be considered to represent the daily mean SSTs, which will be compared with *in situ* daily mean SSTs and discussed further. In Section 2, the satellite SST and *in situ* data used are briefly described. The method is introduced in Section 3. Section 4 explains the processing flow and shows the results. Section 5 gives discussions and conclusions.

2. Data

The specifications of the satellite data used in this study are shown in Table 1. The AVHRR SSTs were produced by the A-HIGHERS system at Tohoku University (Sakaida *et al.*, 2000). The coverage of the A-HIGHERS system is from 120°E to 160°E and 20°N to 60°N (see Fig. 1) and the spatial resolution of the products is 0.01°. The accuracy is about 0.6 K (Sakaida and Kawamura, 1992). GMS S-VISSR hourly SST products were generated at the Sendai Research Center (Tanahashi *et al.*, 2000), which covers the area from 60°S to 60°N and 80°E to 160°W (Fig. 1) and the spatial resolution is 0.05°. The accuracy is 0.8 K. TMI SST products were provided by Earth Observation Research Center (EORC) of National Space Development Agency (NASDA). The spatial resolution of the mapped SST is 0.25° and the accuracy is 0.7 K (Kachi *et al.*, 2001). TRMM Visible and Infrared Scanner (VIRS) level 1B data were provided by EORC and reprocessed at Tohoku University. The 0.05°-mapped SSTs were produced for this study. The accuracy is 0.7 K (Guan *et al.*, 2003). TRMM covers the equatorial and mid-latitude zone between 38°S to 38°N (Fig. 1). It takes about three days to fill the swath gaps and obtain a complete coverage for the TMI zone.

The *in situ* data from three buoys in the sea off Shikoku, the sea of Japan and the East China Sea, deployed by Japan Meteorological Agency (JMA), were used to evaluate the merged SST products. The location

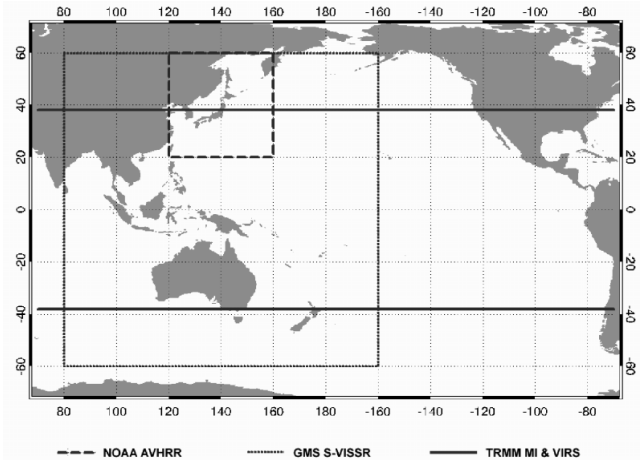

Fig. 1. Coverage of satellite SST products.

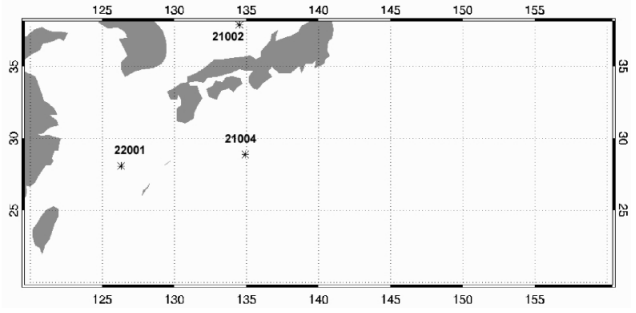

Fig. 2. Location of the JMA buoys.

of the buoys is shown in Fig. 2. SST and other parameters are measured usually every three hours.

The error statistics for each satellite product at three buoy locations are shown in Table 2. The daily-mean satellite SSTs are compared with the daily-mean buoy SSTs for October 1999 to April 2000. Assuming some cloud detection errors, we rejected the match-ups with a difference greater than 3K. For the AVHRR-SST, the satellite SSTs 5×5 pixels centered at the buoy location are averaged. The biases and standard deviations (STDs) of AVHRR and TMI SSTs are consistent with or a little worse than the global statistics shown in Table 1; the STDs of AVHRR SSTs are 0.6–0.7 K, and those of TMI SSTs 0.54 K for the buoy 21004 and 0.99 K for 22001. The TMI STD for the buoy 21002 is 1.78 K. This may be attributed to the fact that the buoy location is around the northern edge of TMI coverage and SSTs colder than 10°C appear in wintertime. It is difficult for the TMI channels to detect SSTs lower than 10°C (e.g. Shibata *et al*., 1999). The STDs of GMS SSTs (0.99–1.07 K) are larger than the global STD of 0.7 K (Table 1). This degradation for the local seas may be caused by the GMS SST algorithm,

Table 2. Error statistics for each satellite product at three buoy locations.

Buoy ID	Sensor	Bias (K)	Std. dev. (K)
21002	AVHRR	–0.16	0.73
	GMS	–0.20	0.95
	TMI	0.43	1.78
21004	AVHRR	–0.32	0.66
	GMS	–0.44	1.07
	TMI	–0.16	0.54
22001	AVHRR	–0.18	0.65
	GMS	–0.61	1.10
	TMI	–0.05	0.99

which is tuned against the *in situ* SSTs in the entire GMS dish coverage (Tanahashi *et al*., 2000).

3. Method

Objective analysis was applied to merge the SST data from infrared and microwave satellites. Based on the Gauss-Markoff theorem, objective analysis was first introduced into oceanographic applications by Bretherton *et al*. (1976). Carter and Robinson (1987) gave a detailed explanation and applications of objective analysis for the estimation of different oceanic fields. The technique has also been applied to satellite remote sensing data. Kelly and Caruso (1990) developed an objective method to generate high resolution wind maps from irregularly spaced scatterometer data and tested it on synthetic data for the northeast Pacific Ocean. An improved objective analysis method was applied to TOPEX/Poseidon and ERS-1 data to generate sea level anomaly maps (Le Traon *et al*., 1998).

Assuming that various data from satellites are available with irregular spatial and temporal gaps, the linear minimum mean square estimation of SST at the location (x, y) at time t is given by (Carter and Robinson, 1987),

$$\hat{\theta}(x,y,t) = CA^{-1}\phi \tag{1}$$

$\hat{\theta}(x, y, t)$ is the estimated SST, ϕ is the matrix of SST data, A^{-1} is the inverse of the autocorrelation matrix between the data, and C is the cross correlation matrix between the estimations and satellite data of SST.

A simple analytical correlation function $C(r)$ was used (Carter and Robinson, 1987).

$$C(r) = \left(1 - r^2\right)\exp\left(-r^2/2\right) \tag{2}$$

$$r^2 = \left(\frac{\Delta x}{L}\right)^2 + \left(\frac{\Delta y}{L}\right)^2 + \left(\frac{\Delta t}{T}\right)^2 \tag{3}$$

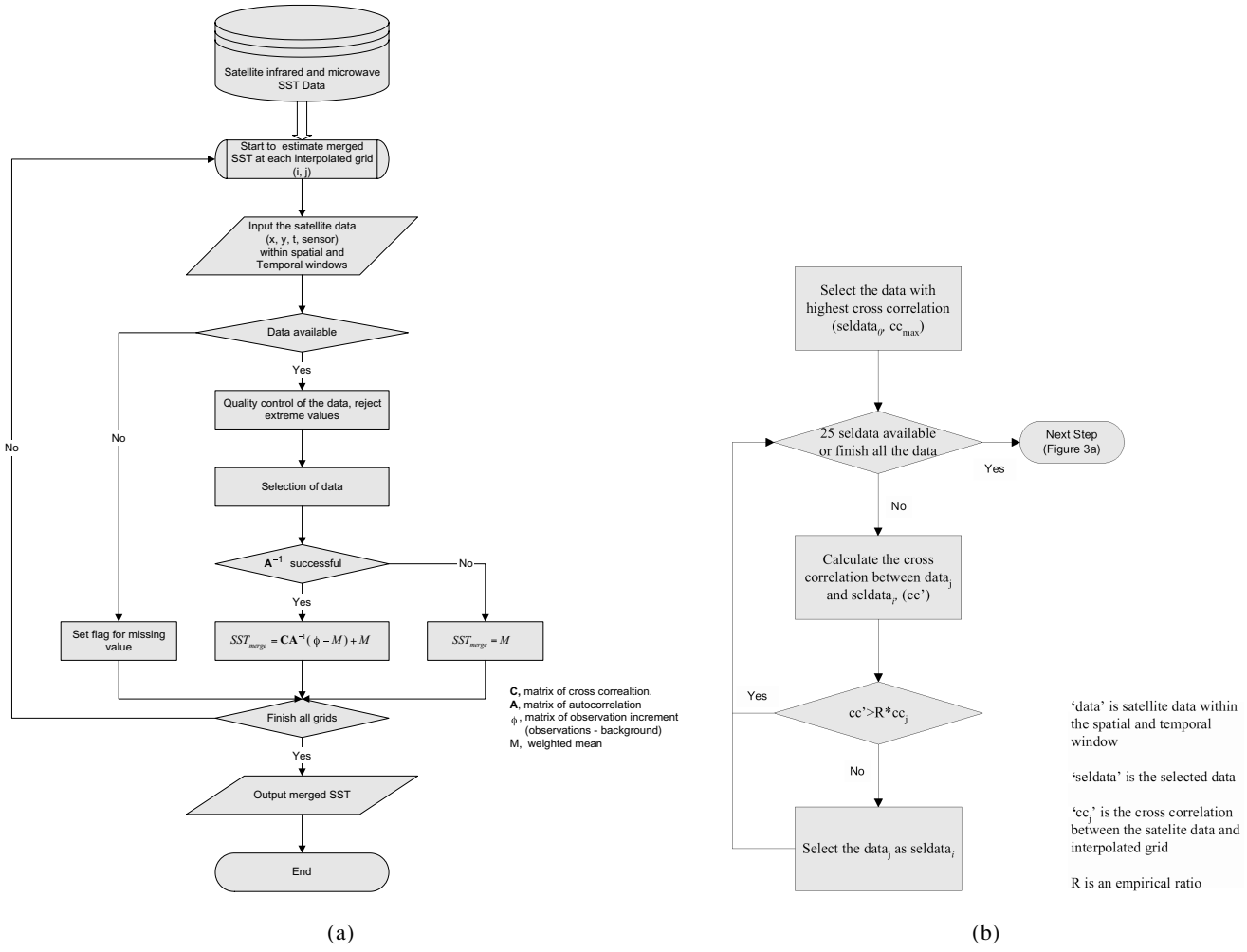

Fig. 3. (a) Flow chart of the process. (b) Flow chart of the data selection.

Δx is zonal distance between the estimation and observation, Δy is meridional distance between the estimation and observation, Δt is temporal difference between the estimation and observation, L and T are spatial and temporal decorrelation scales. In the merging process, we do not use the observation data whose distances from the estimation point are larger than L or whose temporal difference from the estimation time is larger than T.

4. Results

4.1 Merging procedure

Figure 3(a) shows the processing flow diagram for merging the infrared and microwave SST data. Satellite SST data were pre-processed to generate a standard database. The products of different data types were converted to the same 1-byte binary format in order to save space and facilitate the applications in the process. AVHRR and TMI SSTs were resampled to a grid size of 0.05° For AVHRR, all the SST data available in a 5×5 box were averaged. For TMI, a weight function was applied to the three pixels along zonal and meridional direction centered at the resampled pixel in order to approximately correct for the sub-pixel effect.

The grid size of merged SST was set to 0.05°. L and T were set as constant, i.e., 1° and 5 days. In our processing we use three-day data centered at the current day. If Δt is equal two days, we just select the five-day data within the spatial window with the condition that the cross correlation values are positive. For each grid, firstly, quality control was conducted for the input data the locations of which are within 0.5° of the estimated grid. The criterion was set as

$$\left|SST_i - \overline{SST_i}\right| \le 2\,\mathrm{K}. \tag{4}$$

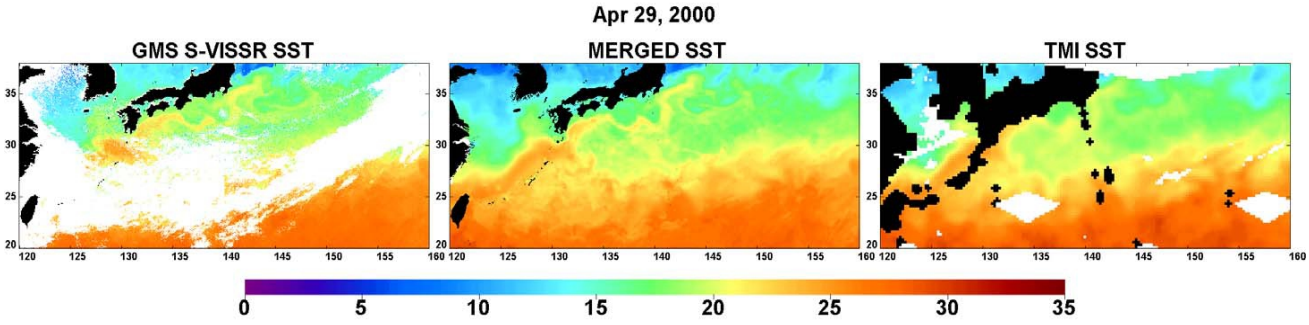

Fig. 4. Comparison of GMS S-VISSR, merged and TMI SST in the Kuroshio region.

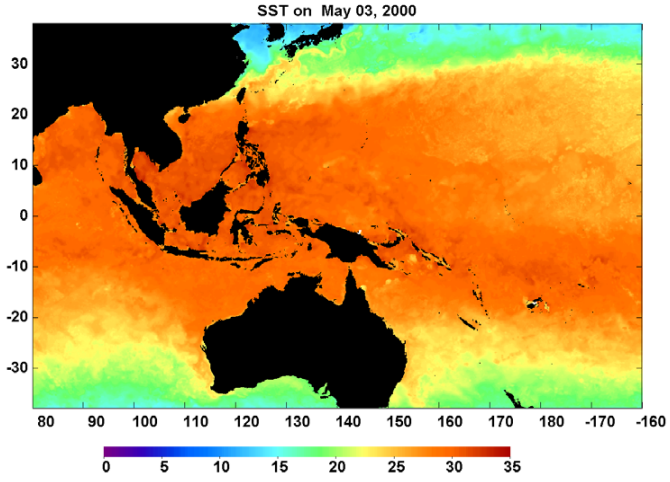

Fig. 5. Merged SST in the Asia-Pacific region

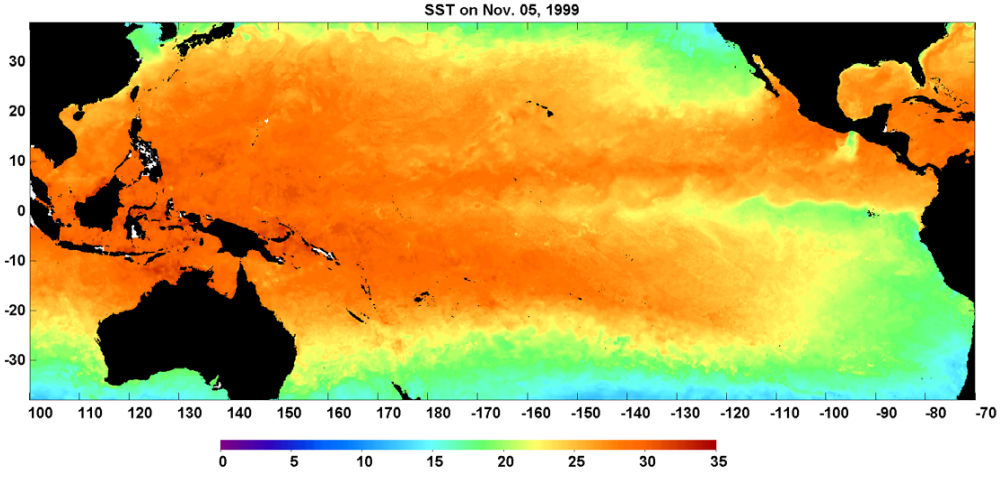

Fig. 6. Merged SST in the Pacific.

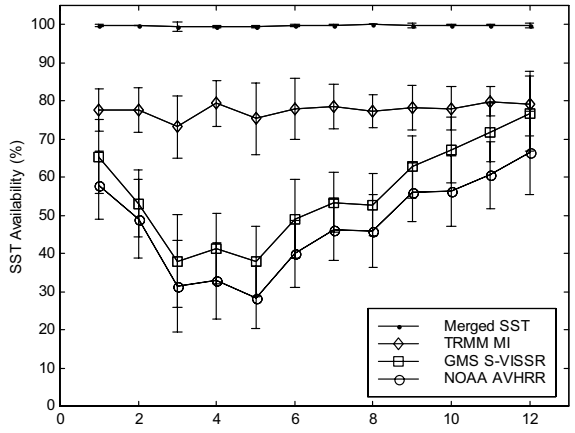

Fig. 7. Comparison of the SST availabilities of Merged SST, TMI, GMS S-VISSR and NOAA AVHRR.

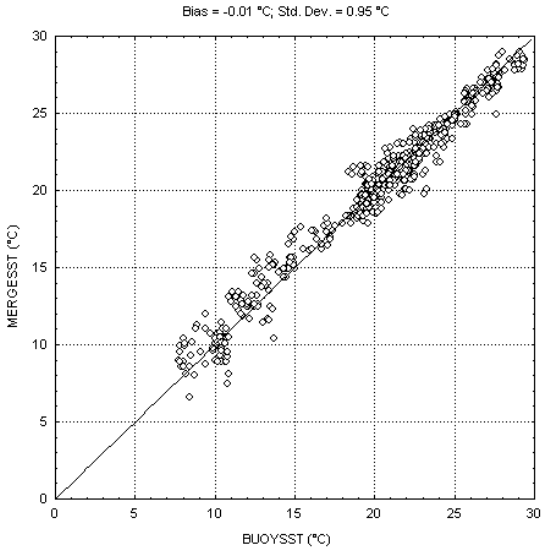

Fig. 8. Comparison of merged and buoy daily-mean SST.

The input SST data which deviate from the mean of these data by greater than 2 K were rejected.

Secondly, for the satellite data, the priority was set as AVHRR (VIRS), TMI, GMS, taking account of SST accuracy and spatial resolution. The SST with the highest priority was selected if several data were available at the same location.

The selected data were sorted by their cross correlation using Eqs. (2) and (3). The procedure of "selection of data" in Fig. 3(a) is explained in detail in Fig. 3(b). Firstly, the data with the highest cross correlation were selected (called A-selected). Then the cross correlation of next data (called B-data) with A-selected was calculated. This cross correlation value was compared with the cross correlation of B-data with the interpolated gird multiplied by an empirical ratio. If the former value is less than the latter value, B-data were selected (B-selected), and rejected otherwise. The next data were compared with all the selected data (A-selected and B-selected). This process was repeated until the number of the selected data reached 25. Hence, in the area of high SST availability, only the data close to the interpolated grid are used.

After the screening of the data, a weighted mean calculated from the selected data was removed from the data. The linear minimum mean square estimator was then applied. The mean was added back after the estimation. If the inverse of the autocorrelation matrix was invalid, the mean value was given for the output.

Satellite infrared and microwave SST data during a one-year period from October 1999 to September 2000 were processed. Merged products were generated in three regions: the Kuroshio region using AVHRR, S-VISSR and TMI SSTs, the Asia-Pacific region using S-VISSR, TMI and VIRS SSTs, and in the Pacific using TMI and VIRS SSTs.

4.2 Evaluation

Comparison of the merged SST with GMS S-VISSR and TMI SST shows the advantages of the merged SST (see Fig. 4). The surface thermal features were interrupted by clouds in the infrared images. Microwave has limited resolution, which obscures fine structure. Combining the infrared and microwave SSTs, the merged SST provides a cloud-free, high-resolution view of the surface thermal structures on April 29, 2000. The fine structure of the Kuroshio was revealed from the merged SST. Figure 5 shows the merged SST in the eastern Indian Ocean and western Pacific and Fig. 6 is a view of SST in the Pacific. The Kuroshio, the Gulf Stream, the Subtropical Fronts, the tropical instability waves, and the upwellings are shown clearly in the daily SST images.

The monthly mean and standard deviation of the SST availabilities from the merged products and individual satellite SST in the Kuroshio region were compared (see Fig. 7). The SST availability of TMI is relatively constant through a year, with the lowest monthly-mean value of 73% in December and highest of 80% in August. The variations of the monthly mean SST availabilities of AVHRR and S-VISSR are very large; the former ranges from 28% in February to 66% in September and the latter from 38% in February to 77% in September (Guan and Kawamura, 2003). However, by merging of the three-sensor SSTs, the availability is above 99%. The unavailability is due to bad observations in the coastal area and persistent rainfall. The annual mean availabilities of the merged, TMI, GMS and NOAA SSTs are 99.8%, 77.6%, 55.8% and 47.6% respectively.

The *in situ* SST data from three JMA buoys (see Fig.

2) were used to evaluate the accuracy of the merged SST products. The study period is from Oct. 1999 to Apr. 2000. Daily mean SSTs were calculated for each buoy. The merged SST corresponding to the location of the buoys was selected. The match-up data were then generated, totaling about 600 cases. Figures 8 shows the comparison of merged and buoy daily mean SSTs. The bias is –0.01 K and standard deviation is 0.95 K.

5. Discussions and Conclusions

The merging of satellite infrared and microwave SSTs has been investigated. The quality of the merged products was evaluated. The preliminary results derived from the objective analysis demonstrate the practicality and advantages of combining of the satellite data.

Taking accounting of the error sources, firstly, a simple analytical correlation function and constant decorrelation scales were used in the objective analysis, which may cause error when satellite data far away from the interpolation grid were used. A more realistic correlation function and variable decorrelation scales will be investigated. However, the time/space dependent decorrelation scales are beyond the scope of the present study. Secondly, the individual satellite SST has error, e.g., the rms error of NOAA AVHRR SST is 0.6 K, those of TMI SST and GMS S-VISSR SST are 0.7 K and 0.8 K respectively. Thirdly, there were spatial and temporal differences between merged and buoy SSTs. The merged SST is the 0.05-degree gridded daily product, while the JMA buoy SSTs are point measurements. The former can be considered a daily mean SST through the present objective analysis, but the buoy-derived daily mean SST is an average of 3-hourly measurements. These differences in observations and processing can be sources of error. Despite these considerable error sources, the standard deviations of the difference between the merged and buoy SST is 0.95 K for daily mean merged SST. Our results demonstrate that it is very promising to generate high-resolution SST combing various satellite data. To improve the products, merging techniques and the consistence of different satellite SSTs will be investigated further.

Acknowledgements

This study was supported by ADEOS and ADEOS-II projects of the National Space Development Agency of Japan, Special Coordination Fund for Promoting Science and Technology "New Generation SST" of MEXT, Japan and Category 7 of MEXT PR2002 Project for Sustainable Coexistence of Human, Nature and the Earth. Dr. Lei Guan's research was also supported by the National Natural Science Foundation of China (Grant No. 40306029). The authors would like to thank EORC of NASDA for the provision of TRMM data and JMA for buoy data.

References

Bretherton, F., R. Davis and C. Fandry (1976): A technique for objective analysis and design of oceanographic experiments applied to MODE-73. *Deep-Sea Res.*, **23**, 559–582.

Carter, E. F. and A. R. Robinson (1987): Analysis models for the estimation of oceanic fields. *J. Atmos. Oceanic. Technol.*, **4**, 49–74.

Donlon, C. J., P. Minnett, C. Gentemann, T. J. Nightingale, I. J. Barton, B. Ward and J. Murray (2002): Towards improved validation of satellite sea surface skin temperature measurements for climate research. *J. Climate*, **15**, 353–369,

Goodrum, G., K. B. Kidwell and W. Winston (2000): NOAA KLM User's Guide September 2000 Revision. NOAA/NESDIS/NCDC.

Guan, L. and H. Kawamura (2003): Study on the SST availabilities of satellite infrared and microwave measurements. *J. Oceanogr.*, **59**, 201–209.

Guan, L., H. Kawamura and H. Murakami (2003): The retrieval of sea surface temperature from TRMM VIRS data. *J. Oceanogr.*, **59**, 245–249.

Kachi, M., H. Murakami, K. Imaoka and A. Shibata (2001): Sea surface temperature retrieved from TRMM Microwave Imager and Visible Infrared Scanner. *J. Meteorol. Soc. Japan* (submitted).

Kawai, Y. and H. Kawamura (2003): Validation of daily amplitude of sea surface temperature evaluated with a parametric model using satellite data. *J. Oceanogr.*, **59**, 637–644.

Kawamura, H. (2002): New Generation Sea Surface Temperature for Ocean Weather Forecasts, Techno-Ocean 02, Kobe Port Island, CD-ROM.

Kelly, K. A. and M. J. Caruso (1990): A modified objective mapping technique for scatterometer wind data. *J. Geophys. Res.*, **95** 13483–13496.

Kidwell, K. B. (1998): NOAA Polar Orbiter Data User's Guide (TIROS-N, NOAA-6, NOAA-7, NOAA-8, NOAA-9, NOAA-10, NOAA-11, NOAA-12, NOAA-13 and NOAA-14) November 1998 Revision. NOAA/NESDIS/NCDC.

Le Traon, P. Y., F. Nadal and N. Ducet (1998): An improved mapping method of multisatellite altimeter data. *J. Atmos. Oceanic. Technol.*, **15**, 522–534.

Legeckis, R. and T. Zhu (1997): Sea surface temperature from the GOES-8 geostationary satellite. *Bull. Amer. Meteor. Soc.*, **78**, 1971–1983.

McClain, E. P. (1989): Global sea surface temperatures and cloud clearing for aerosol optical depth estimates. *Int. J. Remote Sens.*, **10**, 763–769.

Sakaida, F. and H. Kawamura (1992): Estimation of sea surface temperatures around Japan using the Advanced Very High Resolution Radiometer (AVHRR)/NOAA-11. *J. Oceanogr.*, **48**, 179–192.

Sakaida, F., J. Kudoh and H. Kawamura (2000): A-HIGHERS—The system to produce the high spatial resolution sea surface temperature maps of the western north Pacific using the AVHRR/NOAA. *J. Oceanogr.*, **56**, 707–716.

Schlüessel, P., W. J. Emery, H. Grassl and T. Mammen (1990): On the depth skin temperature difference and its impact on satellite remote sensing of sea surface temperature. *J. Geophys. Res.*, **95**, 13341–13356.

Shibata, A., K. Imaoka, M. Kachi and H. Murakami (1999):

SST observation by TRMM Microwave Imager aboard Tropical Rainfall Measuring Mission. *Umi no Kenkyu*, **8**, 135–139 (in Japanese with English abstract)

Strong, A. and E. P. McClain (1984): Improved ocean surface temperautres from space—Comparisons with drifting buoys. *Bull. Amer. Meteor. Soc.*, **65**, 138–142.

Tanahashi S., H. Kawamura, T. Matsuura, T. Takahashi and H. Yusa (2000): Improved Estimates of wide-ranging sea surface temperature from GMS S-VISSR data. *J. Oceanogr.*, **56**, 345–358.

Tanahashi, S., H. Kawamura, T. Takahashi and H. Yusa (2003): Diurnal variations of sea surface temperature over the wide-ranging ocean using VISSR on board GMS. *J. Geophys. Res.*, **108**, 3216.

Wentz, F. J., C. Gentemann, D. Smith and D. Chelton (2000): Satellite measurements of sea surface temperature through clouds. *Science*, **288**, 847–850.

Wu, X., W. P. Menzel and G. S. Wade (1999): Estimation of sea surface temperature using GOES-8/9 radiation measurements. *Bull. Amer. Meteor. Soc.*, **80**, 1127–1138.